Heliyon 9 (2023) e18160

Contents lists available at ScienceDirect

Heliyon

journal homepage: www.cell.com/heliyon

RGFP966 exerts neuroprotective effect via HDAC3/Nrf2 pathway after surgical brain injury in rats

Hai-Ping Gu [a,1], Xiao-Feng Wu [b,1], Ya-Ting Gong [c,1], Mu-Yao Wu [c], Meng-Ying Shi [d], Ya-ming Sun [a,*], Bao-Qi Dang [c,**], Gang Chen [b]

[a] Department of Neurology, Zhangjiagang TCM Hospital Affiliated to Nanjing University of Chinese Medicine, Suzhou, China
[b] Department of Neurosurgery & Brain and Nerve Research Laboratory, The First Affiliated Hospital of Soochow University, Suzhou, China
[c] Department of Rehabilitation, Zhangjiagang TCM Hospital Affiliated to Nanjing University of Chinese Medicine, Suzhou, China
[d] Department of Anesthesiology, Zhangjiagang TCM Hospital Affiliated to Nanjing University of Chinese Medicine, Suzhou, China

ARTICLE INFO

Keywords:
Surgical brain injury
RGFP966
HDAC3
HDAC3/Nrf2 signal pathway
Oxidative stress

ABSTRACT

Background: Histone deacetylase 3 (HDAC3) restores chromatin nucleosomes to a transcriptional repression state, thereby inhibiting gene expression. Studies have found that HDAC3 expression is upregulated in a variety of pathological states of the central nervous system and related to its neurotoxicity. However, the role of HDAC3 in surgical brain injury (SBI) has not been thoroughly explored. Objective: To observe the role of HDAC3 in SBI and the outcome of SBI after its suppression. Methods: Rat SBI model was used, and intraperitoneal injection of RGFP966 (HDAC3 specific inhibitor) was used to detect the changes of HDAC3 expression and neuronal apoptosis indexes in the surrounding cortex of SBI rats, and the cerebral edema and neurological outcome of rats were observed. Results: The expression of HDAC3 in the peripheral cortex of SBI rats was increased, and RGFP966 inhibited the upregulation of HDAC3 and saved the nerve cells around the damaged area. In addition, RGFP966 increased the expression of anti-oxidative stress proteins such as heme oxygenase-1 (HO-1) and superoxide dismutase 2 (SOD2). At the same time, the expression of apoptotic marker protein cleaved-caspase-3 (cle-caspase-3) was decreased, while the expression level of apoptotic protective marker protein B-cell lymphoma 2 (Bcl-2) was increased. In addition, this research demonstrated that in the RGFP966 rat SBI model, the expression level of antioxidant modifier nuclear factor-erythroid 2-related factor 2 (Nrf2) was increased. Conclusion: RGFP966 might activate HDAC3/Nrf2 signaling pathway by inhibiting HDAC3, regulated oxidative stress and nerve cell apoptosis induced by SBI in rat SBI model, reduced brain edema, and had a protective effect on nerve injury. It might be a potential target of SBI pathology.

* Corresponding author. Department of Neurology, Zhangjiagang TCM Hospital Affiliated to Nanjing University of Chinese Medicine, No.77 Changan Southern Road, Suzhou 215600, China
** Corresponding author. Department of Rehabilitation, Zhangjiagang TCM Hospital Affiliated to Nanjing University of Chinese Medicine, No.77 Changan Southern Road, Suzhou 215600, China
E-mail addresses: sunyaming2001@126.com (Y.-m. Sun), zhenjiangdbq@163.com (B.-Q. Dang).
[1] These authors have contributed equally to this work.

https://doi.org/10.1016/j.heliyon.2023.e18160
Received 11 October 2022; Received in revised form 29 May 2023; Accepted 10 July 2023
Available online 12 July 2023

1. Introduction

Surgical brain injury (SBI) is a common and urgent problem in neurosurgery. Secondary brain edema, neuronal cell necrosis and nerve function injury caused by SBI is a complex and interrelated pathophysiological process [1]. Oxidative stress and neuronal cell apoptosis play an important role in secondary brain injury [2]. Oxidative stress promote apoptosis of cystase-dependent cells and thus affect neurological function. Mitochondria are the main source of reactive oxygen species (ROS) under normal physiological conditions, and superoxide radical (O_2^-) is the main ROS produced by this organelle [3]. After brain injury, the large accumulation of ROS

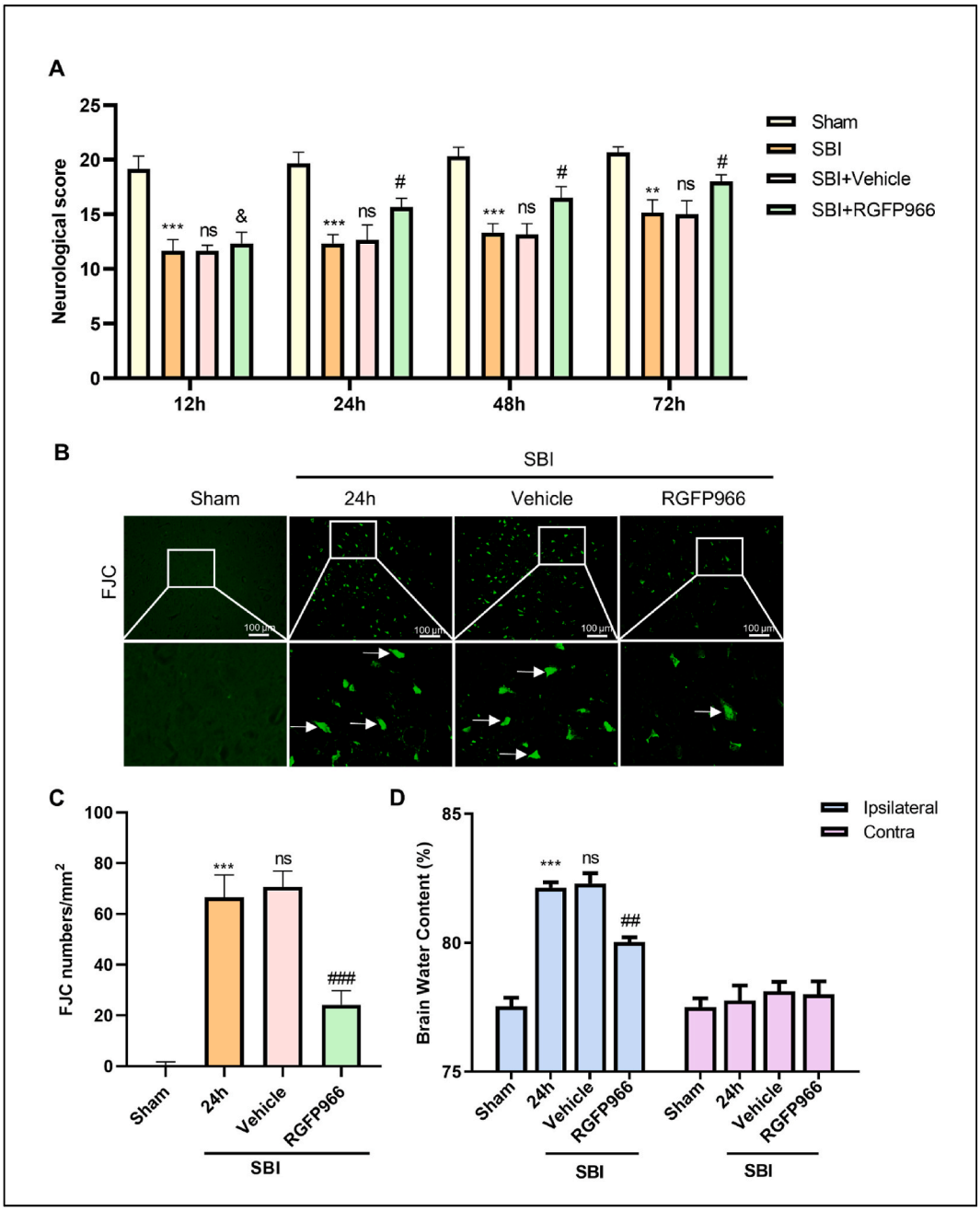

Fig. 1. Neurological function scores, FJC staining and brain edema assessment of different groups. Quantification of neurological scores in the Sham and SBI groups at 12 h, 24 h, 48 h and 72 h after SBI (A). FJC staining in SBI rats after RGFP966 intervention, Scale = 100 μm (B, C). The brain water content of the bilateral hemispheres of the different groups was measured using the wet-dry method (D). Data are presented as the mean ± SD. $^{**}P < 0.01$, $^{***}P < 0.001$ vs. the Sham group; ns $P > 0.05$ vs. the SBI group; & $P > 0.05$, $\#P < 0.05$, $\#\#P < 0.01$, $\#\#\#P < 0.001$ vs. the SBI + Vehicle group. N = 6.

will cause the imbalance of oxidative and antioxidant systems in the body, resulting in oxidative stress, which will cause body damage [4]. Superoxide dismutase (SODs) are the major reactive oxygen scavenging enzyme in cells, which catalyzes the degradation of superoxide radicals O_2^- to hydrogen peroxide (H_2O_2) and molecular oxygen (O_2) [5]. After SBI, the damaged mitochondria release excessive reactive oxygen, deplete the endogenous antioxidant enzymes (such as superoxide dismutase 2 (SOD2)), and regulate the imbalance of oxidative stress, which leads to lipid peroxidation and cytotoxicity, and further oxidative stress and mitochondrial dysfunction [6,7]. Impaired mitochondrial membrane permeability and proteins related to mitochondrial apoptosis can promote caspase-dependent neuronal apoptosis [8]. Therefore, it is very important to find an effective method to reduce the oxidative stress caused by SBI in clinical patients.

Nuclear factor-erythroid 2-related factor 2 (Nrf2) as a known transcription factor, is a member of the basic leucine zipper (bZIP) family of transcription factors [9]. It is an important nuclear factor that has been of primary focus in recent years, and it plays an important role in the nervous system as an important antioxidant regulator [10–12]. It is involved in regulating a series of antioxidants and cytoprotective factors to deal with oxidative stress damage. Under normal conditions, Nrf2 is mainly locates in the cytoplasm and binds to its inhibitor, Kelch-like ECH-related protein 1 (Keap1), which is associated with actin cytoskeleton and promotes Nrf2 to the proteasomal degradation [13]. Under oxidative stress conditions, with the increase of ROS, Nrf2 dissociates from Keap1, reduces degradation, and translocates into the nucleus, and initiates antioxidant genes antioxidant response element (ARE) in the daughter binds to initiate the expression of antioxidant genes, such as heme oxygenase-1 (HO-1), thereby eliminating excess ROS, showing a powerful antioxidant effect [14,15].

The activation of Nrf2/ARE pathway is closely related to histone deacetylases (HDCAs) and histone acetylation levels [16–18]. HDACs work by deacetylation of histones (removing acetyl groups) to wrap DNA more tightly around the histones, making them less accessible to gene transcription factors. Histone deacetylase 3 (HDAC3) is a protein that belongs to class I HDACs in the Histone deacetylase (HDAC) family. It has a high level of expression in the brain and is mainly located in the nucleus of neurons [19,20], and it participates in the deacetylation process of histones, thereby affecting the transcription and expression of target genes [21–23]. Recent studies have shown that HDCA3 can bind to the Nrf2 promoter and inhibit its transcriptional activity, while inhibiting the expression of HDCA3 enhances the expression level of Nrf2 [22,23]. The RGFP966 is an *N*-(*o*-aminophenyl) carboxamide HDAC inhibitor, which can effectively inhibit the expression and function of HDCA3, administration of RGFP966 at a dose of 10 mg/kg resulted in maximum brain exposure between 30 min and 1 h, and the brain concentrations in excess of the IC_{50} of RGFP966 for HDAC3 [24,25]. A substrate-dependent biochemical assay using recombinant human HDACs found that RGFP966 is a specific inhibitor for HDAC3, with an IC_{50} of 0.08 μM [25]. The application of RGFP966 improves the neurological function of many neurological diseases, such as the selective inhibition of the neuroprotective effect of HDAC3 in experimental stroke [26].

Previous researches by our research found that SBI caused brain damage [27], while excessive oxidative stress aggravated brain damage and played an important role in secondary brain injury [6]. It has been reported that HDAC3 is associated with oxidative stress [23]. And so it's reasonable to speculate whether HDAC3 might have the same pathway in surgical brain injury. However, there is no literature to study its effect of inhibition of HDAC3 by RGFP966 on the HDAC3/Nrf2 pathway in the SBI model. This motivated us to explore whether RGFP966 can reduce the brain damage after SBI by inhibiting HDAC3 and activating the protective pathway of Nrf2/ARE.

The hypothesis of this experiment is as follows: RGFP966 inhibits HDAC3, and the reduction of HDAC3 upregulates the expression of Nrf2, thereby increasing the expression of SOD2 and HO-1, which plays a role in anti-oxidative stress and thus achieves the purpose of brain protection.

2. Results

2.1. Effects of RGFP966 intervention on neurobehavioral scores of SBI rats

To evaluate the neurological function of each group, in our study, the SBI group showed the highest neurological deficit 12 h after surgery, and gradually improved thereafter. There were no significant difference between SBI and SBI + Vehicle group at each time node of the experiment. At 24 h after surgery, the SBI + RGFP966 group showed better neurological function for the first time than the SBI + Vehicle group ($P < 0.05$). (Fig. 1A).

2.2. Effects of RGFP966 intervention on neurodegenerative death and brain edema after SBI

Our research showed that the degree of degeneration and necrosis of nerve cells in the SBI group was significantly greater than that in the Sham group ($P < 0.001$); there was no significant difference in the degree of degeneration and necrosis of nerve cells in the SBI group and the SBI + Vehicle group ($P > 0.05$); and after RGFP966 intervention, the degree of degeneration and necrosis in the SBI + RGFP966 group was significantly lower than that of the SBI + Vehicle group ($P < 0.001$) (Fig. 1B and C). Brain water content was a key indicator for evaluating the prognosis after SBI [28]. Compared with the sham group, the brain water content of the SBI group was significantly increased ($P < 0.001$), while the intervention of RGFP966 was significantly lower than that of the SBI + Vehicle group ($P < 0.01$). (Fig. 1D).

2.3. RGFP966 inhibits the expression of HDAC3 in diseased cortical neurons

Immunofluorescent evaluation results proved that compared with the Sham group, SBI enhanced the expression of HDAC3 in

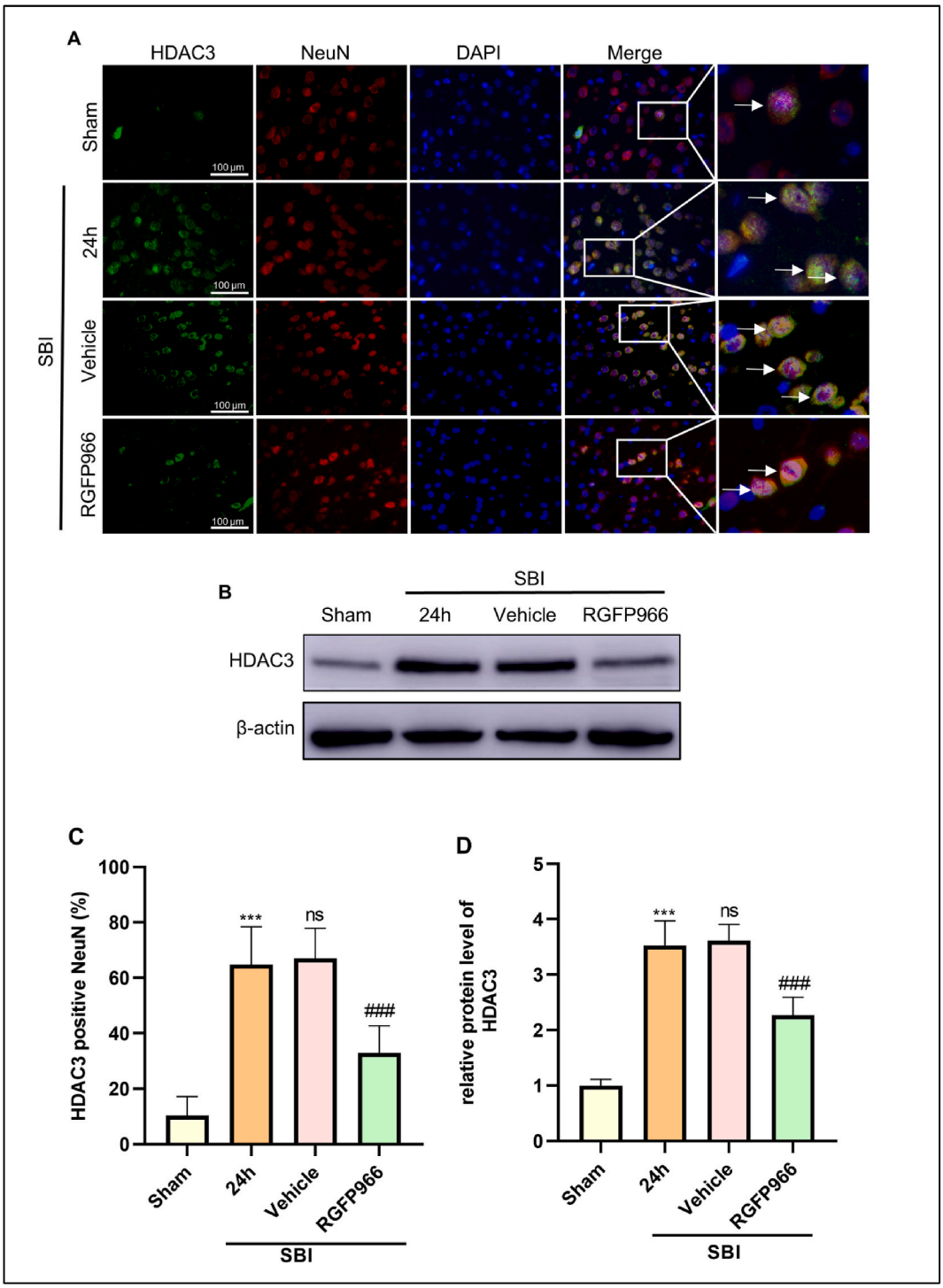

Fig. 2. HDAC3 and neuron nuclei co-staining results and HDAC3 expression in each group after RGFP966 intervention. Representative double-immunofluorescent staining images of green-marked HDAC3 and red-marked NeuN neurons to show expression profiles in Sham, SBI, SBI + Vehicle and SBI + RGFP966 groups. The nuclei were fluorescently labeled with DAPI (blue) (A, C); Scale = 100 μm. Western blotting was used to detect HDAC3 in Sham, SBI, SBI + Vehicle and SBI + RGFP966 groups (B, D). Protein levels were normalized to that of β-actin; Data are presented as the mean ± SD. ***$P < 0.001$ vs. the Sham group; ns $P > 0.05$ vs. the SBI group; ###$P < 0.001$ vs. the SBI + Vehicle group. N = 6.

neurons ($P < 0.001$), and compared with the SBI + Vehicle group, RGFP966 treatment could inhibit the reversal of this trend ($P < 0.001$), (Fig. 2A and C). The change trend of HDAC3 was further verified in Western blot. HDAC3 levels were normalized to β-actin levels, and the data for the four experimental groups were presented as the mean ± standard deviation (SD) as follows:1.00 ± 0.11, 3.53 ± 0.44, 3.61 ± 0.29, 2.67 ± 0.32. Compared with the Sham group, the expression of HDAC3 in the SBI group increased ($P < 0.001$), but there was no significant difference between the SBI group and the SBI + Vehicle group ($P > 0.05$). The expression level of HDAC3 in the SBI + RGFP966 group was lower than that in the SBI + Vehicle group ($P < 0.001$). (Fig. 2B and D).

2.4. The effect of RGFP966 intervention on neuronal apoptosis after SBI

The analysis of terminal deoxynucleotidyl transferase dUTP nick end labeling (TUNEL) staining results confirmed that compared with the Sham group, neuronal apoptosis increased after SBI ($P < 0.001$). Compared with the SBI group, there was no significant change in vehicle intervention ($P > 0.05$), while the TUNEL positive cells in the SBI + RGFP966 group significantly reduced compared with the SBI + Vehicle group ($P < 0.001$) (Fig. 3A and B). This result was further confirmed by subsequent Western blotting. Bcl-2 levels were normalized to β-actin levels, and the data for the four experimental groups were presented as the mean ± SD as follows: 1.00 ± 0.03, 0.44 ± 0.06, 0.45 ± 0.03, 0.61 ± 0.09, and cle-caspase-3 levels were presented as follows: 1.00 ± 0.20, 2.05 ± 0.35, 2.02 ± 0.30, 1.30 ± 0.24. It is observed that after injury, compared with the Sham group, the anti-apoptotic factor Bcl-2 in the lesion area in the SBI group was consumed ($P < 0.001$), and the expression of apoptotic factor cle-caspase-3 increased ($P < 0.001$). Compared with the SBI + Vehicle group, the expression of Bcl-2 in the SBI + RGFP966 group increased ($P < 0.001$), while the expression of cle-caspase-3 decreased ($P < 0.01$) (Fig. 3C–E). These results indicate that RGFP966 does have a neuroprotective effect on the diseased cortex after SBI.

2.5. RGFP966 increases the expression of antioxidant factors by activating the HDAC3/Nrf2 signaling pathway

In this experiment, western blotting was used to detect the levels of Nrf2, SOD2 and HO-1 (Fig. 4A). Nrf2 levels were normalized to β-actin levels, and the data for the four experimental groups were presented as the mean ± SD as follows: 1.0 ± 0.20, 1.48 ± 0.20, 1.47 ± 0.26, 2.08 ± 0.42 (Fig. 4B), SOD2 levels were presented as follows: 1.00 ± 0.05, 0.48 ± 0.05, 0.54 ± 0.08, 0.72 ± 0.10 (Fig. 4D) and HO-1 levels were presented as follows: 1.00 ± 0.31, 1.70 ± 0.35, 1.71 ± 0.24, 2.43 ± 0.44 (Fig. 4C). Western blotting results showed that, compared with the Sham group, the endogenous antioxidant enzyme SOD2 depletion decreased after SBI in rats ($P < 0.001$), but the levels of Nrf2 increased ($P < 0.05$), and antioxidant factor HO-1 also increased ($P < 0.05$). There was no difference between the SBI + Vehicle group and SBI group. After RGFP966 intervention, compared with the SBI + Vehicle group, the SOD2 expression in the SBI + RGFP966 group was reversed and the level increased ($P < 0.01$), and Nrf2 increased further ($P < 0.01$), antioxidant factor HO-1 also increased further ($P < 0.01$) (Fig. 4). The above results indicate that the intervention of RGFP966 activates the HDAC3/Nrf2 signaling pathway and increases the expression of antioxidant factors (Fig. 5).

3. Discussion

Our research proved that the high selective HDAC3 inhibitor RGFP966 [25]had an inhibitory effect on HDAC3 in experimental rat SBI models, it could significantly reduce nerve function injury, brain edema, nerve cell apoptosis and neurodegenerative death induced by SBI in rats. In addition, our research found that the use of RGFP966 activated the Nrf2 pathway and its downstream antioxidant HO-1, SOD2 levels increased, antioxidant capacity was enhanced, and SBI-induced oxidative stress damage was reduced. In our study, at the time point 24 h after SBI in rats, a significant difference in the neurological score between the RGFP966 treatment group and the vehicle group was first discovered (Fig. 1A). And this time point was early enough to look at the processes we were most interested in based on HDAC3 function, especially oxidative stress and apoptosis. Therefore, our research choosed to measure and compare relevant indicators 24 h after SBI.

HDAC3 mainly exists in the nucleus of neurons [29]. HDAC3 levels increase in a variety of animal models of acute central nervous system injury and is proved to be neurotoxic [17,23,24]. RGFP966 competitive tight-binding inhibitors target class I HDACs, with the greatest inhibition of HDAC3, it can effectively inhibit the expression and function of HDCA3 [25]. Our research got the same result. After rat SBI, HDAC3-positive neurons increased significantly in immunofluorescence, and the Western blotting results also showed that HDAC3 levels were upregulated. Compared with the SBI + Vehicle group, the intervention of RGFP966 was effective, and the expression of HDAC3 decreased significantly (Fig. 2). In addition, in a study of cerebellar granule neurons, overexpression of HDAC3 can lead to cell death, and knockout of HDAC3 has a protective effect on neuronal death caused by low potassium [30]. The toxicity induced by HDAC3 is cell-specific, and is the most sensitive to neurons [30]. In our experiment, the neuroprotective effect of the RGFP966 treatment group has also been fully demonstrated, including the decrease in the neurodegeneration, the brain edema, the number of TUNEL positive cells, the increased B-cell lymphoma 2 (Bcl-2) and the down-regulated cle-caspase3 (Fig. 1B–D, Fig. 3). Although the exact mechanism of its neuroprotective and anti-apoptotic properties has not been fully elucidated, it can be speculated that it may be related to the effective inhibition of HDAC3 by RGFP966 and the restoration of its ability to resist oxidative stress, so it can prevent mitochondrial dysfunction caused by SBI.

SBI represents a continuous pathological process. Oxidative stress is a key factor in the pathophysiology of SBI and mediates subsequent histopathology and neurobehavioral defects [7,31]. The balance between oxidative stress and antioxidant factors is crucial for nerve damage [32–34]. After SBI, the levels of oxidation rise [7], which exceeds the capacity of the antioxidant defense system. An unbalanced oxidative system can cause damage to cellular components such as protein, lipids, and DNA, thereby intensifying neuronal

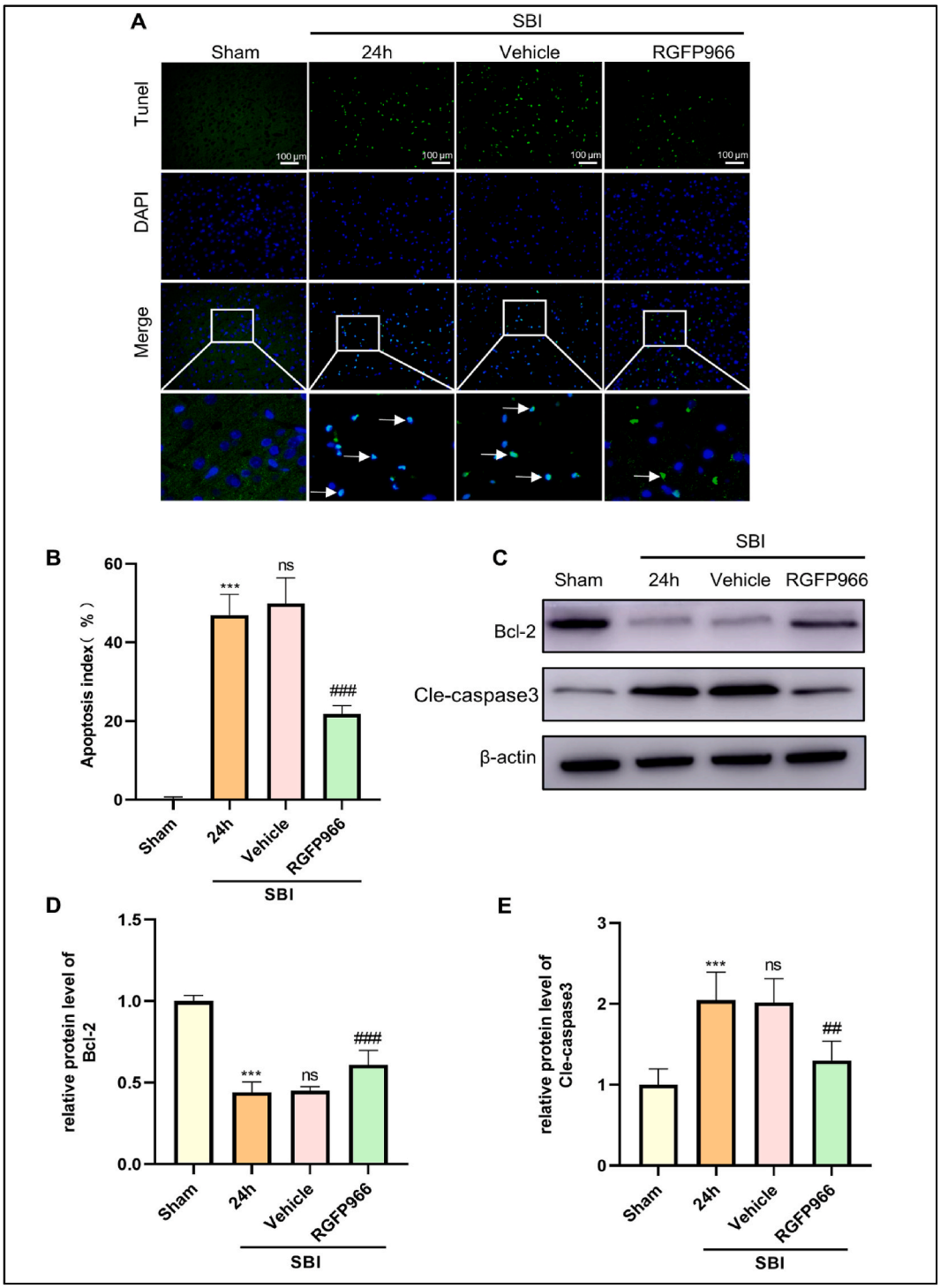

Fig. 3. Evaluation of neuronal apoptosis and expression of apoptosis-related factors after RGFP966 intervention. TUNEL staining, Scale = 100 μm (A, B). Western blot was used to detect Bcl-2 and cle-caspase3 levels of Sham, SBI, SBI + Vehicle and SBI + RGFP966 groups (*C*–E). Data are presented as the mean ± SD. ***$P < 0.001$ vs. the Sham group; ns $P > 0.05$ vs. the SBI group; ##$P < 0.01$, ###$P < 0.001$ vs. the SBI + Vehicle group. N = 6.

apoptosis [35,36]. Therefore, oxidative stress may be a new therapeutic target in SBI. Superoxide dismutase 2 (SOD2) that our concern is the main endogenous antioxidant enzyme, and it is a marker of mitochondrial oxidative stress level. It has a strategic location in the mitochondrial matrix, and is considered to be the first to protect mitochondria from oxidation/nitrative damage Line defense, which is

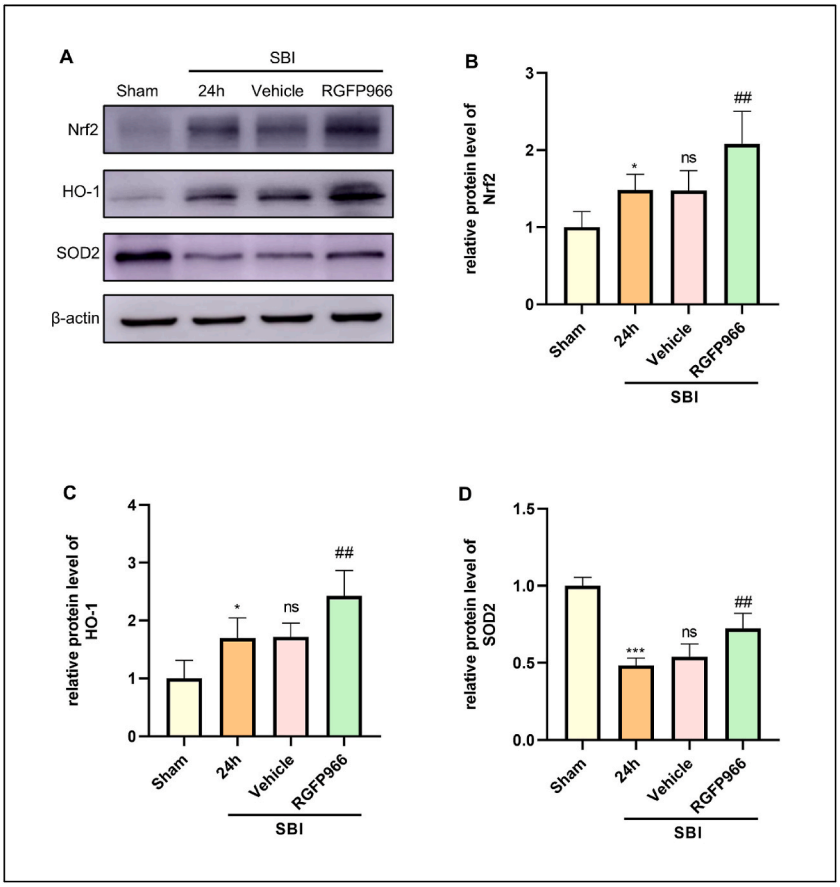

Fig. 4. Expression level of Nrf2 and oxidative stress-related factors after RGFP966 intervention. Western blot was used to detect Nrf2, HO-1 and SOD2 levels in Sham, SBI, SBI + Vehicle and SBI + RGFP966 groups (A–D). Data are presented as the mean ± SD. $*P < 0.05$, $***P < 0.001$ vs. the Sham group; ns $P > 0.05$ vs. the SBI group; $\#\#P < 0.01$ vs. the SBI + Vehicle group. N = 6.

responsible for scavenging the metabolites produced by free radicals, catalyzing the conversion of peroxides into non-toxic forms, protecting cells from oxidative stress [5,6]. 24 h after SBI, the SOD2 content in the brain tissue of the damaged area thatby Western blot was reduced. Compared with the SBI + Vehicle group, RGFP966 treatment significantly reversed this trend, The expression level of SOD2 was significantly upregulated (Fig. 4A, D). This reflected the antioxidant capacity of RGFP966 in the SBI rat model, which might be through the inhibition of HDAC3.

Nrf2 is an important antioxidant regulator that can balance the level of oxygen free radicals. Nrf2 is essential in the induction of antioxidant enzymes, just as in various central nervous system conditions [11,23,37]. A large amount of evidence shows that Nrf2 is a key translation factor that maintains cell redox balance in brain injury to resist oxidative stress. Increased levels of Nrf2 can induce the expression of its downstream antioxidant enzyme HO-1 and reduce oxidative stress damage [11]. HO-1 catalyzes the conversion of the pro-oxidant heme into bilirubin, which has been shown to have strong antioxidant properties [38]. Previous studies have revealed that the transcription of Nrf2 is related to HDAC3 [16–18]. HDCA3 can bind to the Nrf2 promoter and inhibit its transcriptional activity, while inhibiting the expression of HDCA3 enhances the transcription and expression level of Nrf2. Our research had obtained similar results. After SBI, the administration of RGFP966 successfully inhibited the expression of HDAC3, so that the inhibition of Nrf2 was lifted, the expression level of Nrf2 was increased, and the level of its downstream antioxidant factor HO-1 was significantly increased (Fig. 4A–C). These results indicated that RGFP966 could increase the expression of antioxidant factors by activating the HDAC3/Nrf2 signaling pathway.

In Conclusion, this study showed that RGFP966 acts by activating the HDAC3/Nrf2 signaling pathway. By reducing the action of HDAC3, RGFP966 increased the expression of Nrf2, improved nerve function, reduced brain edema, apoptosis and oxidative stress, thereby reduced the brain damage of SBI (Fig. 5). The data obtained in this study maked RGFP966 an attractive target in future SBI treatments.

This study had some limitations. First, some other Nrf2 upstream factors also had an important influence on the Nrf2 pathway. Further research should investigate whether these signaling pathways were also involved in Nrf2 activation induced by RGFP966 by inhibiting HDAC3. Second, the activation mode of Nrf2 was mainly to translocate from the cytoplasm to the nucleus, reducing the degradation of the pantothenic acid pathway. Our research only observes the change of its total amount, and lacks research on the

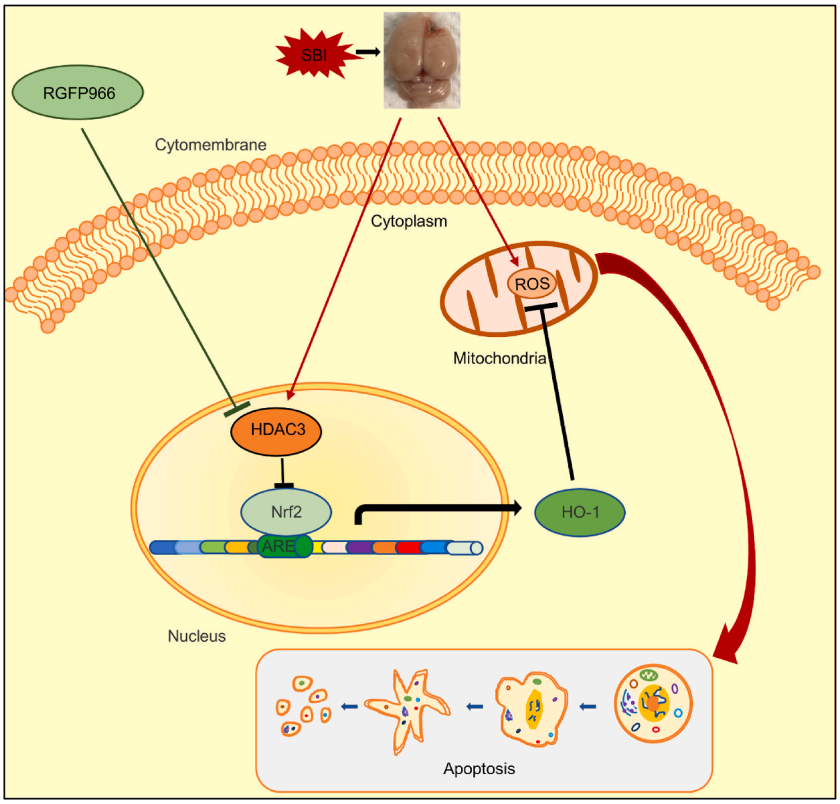

Fig. 5. Mechanism diagram RGFP966 plays a neuroprotective role in surgical brain injury through the HDAC3/Nrf2 pathway. SBI induces a rapid increase of endogenous HDAC3 expression and blocks the Nrf2 pathway. RGFP966 reversed the trend of increased oxidative stress and apoptosis of nerve cells after SBI, and alleviated nerve injury. Arrows indicate activation; Bars represent suppression.

change trend of its cytoplasm and nucleus content. Third, studies have confirmed that RGFP966 can down-regulate the expression level of HDAC3 and inhibit its activity in vivo and in vitro experiments [17,39]. Our research only observed the expression level changes of HDAC3 after the application of RGFP966, and there was no study on its activity. Therefore, we should make up for the above deficiencies in the further study.

4. Experimental procedure

4.1. Animals

Male Sprague-Dawley rats (300–350 g) were kept under controlled environmental conditions with a light/dark cycle of 12 h and free access to sufficient food and water [40]. These rats were purchased from Zhaoyan (Suzhou) New Drug Research Center. All procedures involving animals have been approved by Institute of Animal Care Committee of Zhangjiagang Traditional Chinese Medicine Hospital and all operations comply with the National Institutes of Health (NIH) guidelines for the Care and Use of Laboratory Animals.

4.2. Study design and experimental groups

Two separate experiments (Fig. 6).

Experiment 1: In order to determine the earliest node for RGFP966 to improve the neurological function of SBI, 24 experimental rats (24 of 25 rats survived) were randomly divided into Sham group, SBI group, SBI + Vehicle group, SBI + RGFP966 group, with 6 experimental rats in each group. Rats were given neurological function scores at 12 h, 24 h, 48 h, and 72 h after surgery. After last neurological evaluation, all experimental rats were euthanized [41] (Fig. 6B). All experimental procedures were carried out blind.

Experiment 2: To determine the role of HDAC3 in SBI and its possible mechanism, 48 experimental rats (48 of 51 rats survived) were randomly divided into Sham group, SBI group, SBI + Vehicle group, SBI + RGFP966 group, with 12 experimental rats in each group. According to the results of experiment 1, rats were sacrificed 24 h after SBI and brain tissue was taken out. 6 rats in each group were used for brain water content detection, and another 6 rats were used for Western blot analysis and staining [42] (Fig. 6C). All experimental procedures were carried out blind.

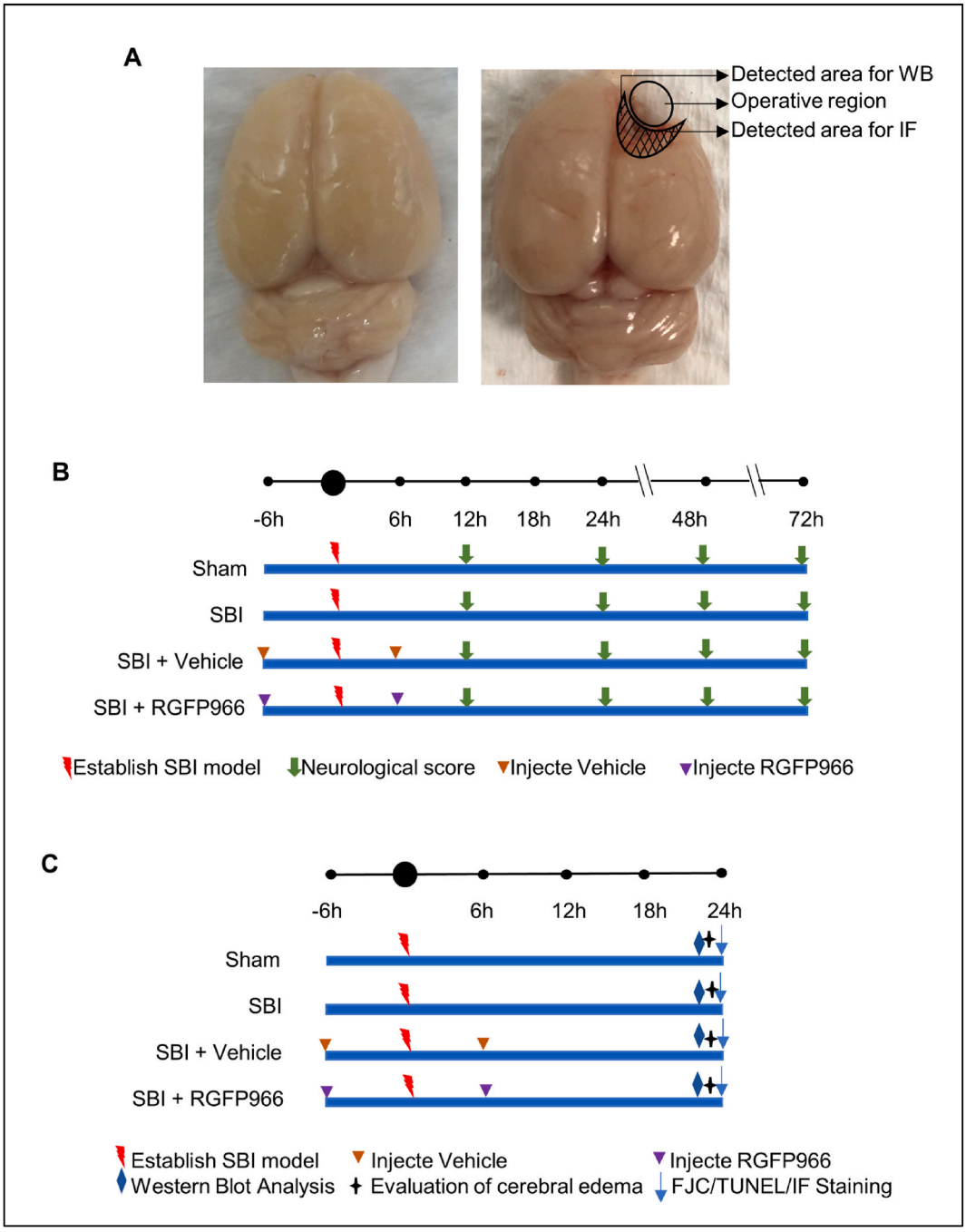

Fig. 6. Representative brain maps and technical roadmaps of different groups. Brain tissue from the peripheral injury in the SBI group and from the same location in the sham group was obtained for the assay(A). Experiment 1 was designed to determine the earliest node for RGFP966 to improve the neurological function after SBI and determine a suitable time point for the second experiment (B). Experiment 2 was designed to observe the effects of HDAC3 on early brain injury after SBI and explore the potential mechanisms(C).

4.3. Establishment of experimental rat SBI model

As[2] previously reported [43], our research used the method of partially excising the right frontal lobe of rats to establish an SBI model. After weighing, the experimental rats were anesthetized by intraperitoneal injection of sodium pentobarbital (10 ml/kg). After the anesthesia was successful, skin preparation was performed in the cut area. Then, it was placed on the brain stereotaxic device (Yuyan, China), and disinfected cut area with 1% iodophor, cut the top of the skull and separated the periosteum, a bone window with a diameter of about 5 mm was opened on the right side of the midline 2 mm and 2 mm before the right bregma. The frontal lobe in the exposed area is removed, the bleeding is stopped, disinfected, and finally the wound was closed by suture. In the Sham group, the same operation method was performed, but the right frontal lobe was exposed without resection, and the bleeding was stopped and sutured.

4.4. Drug injection

The SBI + RGFP966 group was administered intraperitoneal injection of RGFP966 (10 mg/kg, dissolved in 10% DMSO; Biorbyt, US) 6 h before and after SBI. The SBI + Vehicle group with matching body weight was injected with the same amount of 10% DMSO at the time point required by the experiment. The dose of RGFP966 used in this study was selected based on previous studies, which showed that there is an effective HDAC3 inhibitory concentration in the brain [24,25].

4.5. Tissue collection and sectioning

Tissue was collected and sectioned as described previously [41]. Before the operation, all experimental rats were anesthetized with sodium pentobarbital via intraperitoneal injection at the time points required by each group. After successful anesthesia, the heart was perfused with 20 ml of 4 °C 0.9% sodium chloride injection, the brain tissue was taken out, and a cortical sample within 3 mm of the edge of the injured area was collected (Fig. 6A). The obtained brain tissue sample was immediately frozen and stored at −80 °C until the target protein content was detected by western blotting. The brain tissue used to make the paraffin section (Fig. 6A) was immersed in 4% paraformaldehyde at 4 °C. All operations were completed within 5 min, and all operations were performed on ice. After the brain tissue was soaked for 48 h, it was embedded in paraffin by two unsuspecting pathologists and cut with a paraffin microtome to make pathological sections for various staining.

4.6. Western blot analysis

Extract brain tissue protein as previously reported [44]: placed an appropriate amount of brain tissue in radio immunoprecipitation assay lysis (RIPA) buffer containing protease inhibitor mixture (Beyotime, China), homogenized at 60 Hz*60 s, and then incubated on ice for lysis for 20 min. Then centrifuged at 4 °C*12,000 g for 20 min, collected an appropriate amount of supernatant, and detected the protein concentration of the extracted protein using the bicanoic acid (BCA) method and Pierce™ BCA protein detection kit (Thurse Fisher, USA). Electrophoresis: Loaded equal amounts of protein into each lane, separate with 10% sodium dodecyl sulfate (SDS) gel (BIO-RAD, USA), load and electrophoresis. Transfer membrane: the to polyvinylidene fluoride (PVDF) membrane (Millipore, USA) immediately after electrophoresis. Sealing: After the transfer, the strip was sealed in QuickBlock™ West (Beyotime, China) at room temperature for 40 min. Incubate the primary antibody: After blocking, incubated with the primary antibody of the target molecule overnight in a refrigerator shaker at 4 °C. Washed three times with TBST. Incubation of the secondary antibody: Used the corresponding secondary antibody to incubate at room temperature for 1 h, and then wash three times with TBST. Finally, added an appropriate amount of super-sensitive luminescent liquid (Millipore, USA) to the strip for exposure and performed chemiluminescence imaging. Used ImageJ software (National Institutes of Health) to analyze the ratio of the gray value of the target band. The primary antibodies used were as follows: HDAC3 (1:1000, Cell Signaling Technology, USA), Nrf2 (1:1000, Abcam, UK), HO-1 (1:1000, Abcam, UK), SOD2 (1:1000, Abcam, UK), Bcl-2 (1:1000, Abcam, UK), Cle-caspase3 (1:1000, Abcam, UK), β-actin (1: 1000, Cell Signaling Technology, USA). The secondary antibodies used are as follows: anti-mouse IgG-HRP (1:1,000, Cell Signaling Technology, USA), anti-rabbit IgG-HRP (1:1,000, Invitrogen, USA).

4.7. Immunofluorescence staining

As previously reported [45] the prepared paraffin sections of brain tissue were baked in an oven at 70 °C for 1 h, and then immersed in xylene, gradient alcohol and citric acid in sequence. Perforate with 0.2% Trition (Beyotime, China), washed 3 times with PBS (Beyotime, China), blocked with immuno-blocking solution for brain department for 30 min, added primary antibody, incubated overnight in a refrigerator at 4 °C, wash 3 times with PBS, added secondary fluorescent antibody, Incubate for 1 h at room temperature, washed 3 times with PBS, mounted the tablet with 4,6-diamino-2-phenylindole (DAPI) anti-fluorescence quenching solution (YEASEN, China), observed and collected images under a fluorescent microscope (OLYMPUS, Japan). The primary antibodies used were as follows: HDAC3 (1:100, Cell Signaling Technology, USA), NeuN (1:200, Abcam, UK). The secondary antibodies used were as follows: donkey anti-mouse IgG antibody, Alexa Fluor 488 (1:500, Invitrogen, USA), donkey anti-rabbit IgG antibody, Alexa Fluor 555 (1:500,

[2] In the cranium angle, the pressure inside the head changes, the brain comes into contact with the foreign air, light and sound … although the changes in the brain caused by these physical forces are not taken into account by surgeons, there will be issues to be considered in the future.

Invitrogen, USA).

4.8. TUNEL staining

Perform TUNEL staining to detect apoptosis (Beyotime, China) according to previous reports [41]. The paraffin removal procedure was the same as before. Cleaned with distilled water for 2 min, then transferred to proteinase K working solution and incubated for 30 min. Washed three times with PBS. The tissue sections were immersed in TUNEL working solution and incubated in a humidified chamber at 37 °C, protected from light, for 1 h. Washed three times with PBS, then mounted the slides with DAPI. Under the fluorescence microscope, green fluorescence staining showed DAPI-stained tunel-positive cell nuclei, and the image was collected.

4.9. Fluoro - jade C staining

Fluoro - Jade C saining (FJC) (Biological Sensis, USA) staining was used to investigate neurodegeneration according to previous reports [46]. Paraffin sections of brain tissue were placed in a 70 °C oven for 1 h, then soaked in xylene, gradient ethanol series, and then rinsed twice with double steaming water for 2 min each time. The slices were transferred to solution C diluted by 10 times for 30 min. Then rinsed with double steam water three times and dried in an oven at 60° Celsius for 10 min. Finally, soaked in xylene for 5 min. After being removed and dried, the slices were sealed with neutral resin (YEASEN, China) and collected under a fluorescence microscope.

4.10. Neurological score

According to previous reports [28], blind observers used the 21-point sensorimotor scoring system to evaluate neurological scores in all experimental rats at the time notes formulated by the experiment. This test includes: (i) spontaneous activity; (ii) symmetry of limb movement; (iii) forelimb extension ability; (iv) sideways turning; (v) climbing ability; (vi) proprioception; (vii)Vibration tactile response. The score given to each rat at the end of the evaluation was the sum of the scores of all test parts. The higher the score, the less nerve damage.

4.11. Evaluation of cerebral edema

The rat brain was taken out under anesthesia 24 h after the operation. According to previous reports [47], the wet-dry method was used to assess the water content of the brain. After the brain tissue was taken out, the olfactory bulb, cerebellum and lower brain stem were removed, and the left and right brains were separated and quickly weighed to determine their wet weight. The brain tissue was then loaded into EP tubes and stored in a refrigerator at −80 °C for later use. After the final brain tissue was weighed, the brain tissue previously stored in the −80 °C refrigerator was removed. Then put these brain tissue in the oven and baked it at 100 °C for 24 h until constant weight, and then weighed it to get the dry weight. Brain water content (%) = [(wet weight-dry weight)/wet weight] × 100%.

4.12. Statistical analysis

All data were expressed as mean ± standard deviation (SD) and analyzed with GraphPad Prism 8.0 (USA) software. One-way analysis of variance (ANOVA) was used for multiple comparisons to explain the differences between groups. $P < 0.05$ was considered statistically significant.

Author contributions

Hai-Ping Gu, Xiao-Feng Wu, Ya-Ting Gong: Performed the experiments; Wrote the paper.
Mu-Yao Wu and Meng-Ying Shi: Performed the experiments.
Ya-ming Sun: Analyzed and interpreted the data; Wrote the paper.
Bao-Qi Dang, Gang Chen: Conceived and designed the experiments; Contributed reagents, materials, analysis tools or data; Wrote the paper.

Data availability statement

No data was used for the research described in the article.

Declaration of competing interest

The authors declare that they have no known competing financial interests or personal relationships that could have appeared to influence the work reported in this paper.

Acknowledgements

This work is supported by the Suzhou Science and Technology Development Plan (SYSD2020003), Gusu Health Talent Training Project (GSWS2020104), Suzhou Science and Technology Development Project (SYS2019002), Zhangjiagang Youth Science and Technology Project (ZJGQNKJ202011), and Zhangjiagang Science and Technology Project (ZKS2020).

References

[1] Y. Xiao, G. Li, Y. Chen, Y. Zuo, K. Rashid, T. He, H. Feng, J.H. Zhang, F. Liu, Milk fat globule-epidermal growth factor-8 pretreatment attenuates apoptosis and inflammation via the integrin-β3 pathway after surgical brain injury in rats, Front. Neurol. 9 (2018) 96.
[2] S. Fu, X. Luo, X. Wu, T. Zhang, L. Gu, Y. Wang, M. Gao, Y. Cheng, Z. Xie, Activation of the melanocortin-1 receptor by NDP-MSH attenuates oxidative stress and neuronal apoptosis through PI3K/Akt/Nrf2 pathway after intracerebral hemorrhage in mice, Oxid. Med. Cell. Longev. 2020 (2020), 8864100.
[3] K.M. Holmström, T. Finkel, Cellular mechanisms and physiological consequences of redox-dependent signalling, Nat. Rev. Mol. Cell Biol. 15 (6) (2014) 411–421.
[4] Y. Zhou, H.D. Wang, X.M. Zhou, J. Fang, L. Zhu, K. Ding, N-acetylcysteine amide provides neuroprotection via Nrf2-ARE pathway in a mouse model of traumatic brain injury, Drug Des. Dev. Ther. 12 (2018) 4117–4127.
[5] A.K. Holley, V. Bakthavatchalu, J.M. Velez-RomanD, K. St Clair, Manganese superoxide dismutase: guardian of the powerhouse, Int. J. Mol. Sci. 12 (10) (2011) 7114–7162.
[6] J. Fang, H. Wang, J. Zhou, W. Dai, Y. Zhu, Y. Zhou, X. Wang, M. Zhou, Baicalin provides neuroprotection in traumatic brain injury mice model through Akt/Nrf2 pathway, Drug Des. Dev. Ther. 12 (2018) 2497–2508.
[7] J.M. Eckermann, W. Chen, V. Jadhav, F.P. Hsu, A.R. Colohan, J. Tang, J.H. Zhang, Hydrogen is neuroprotective against surgically induced brain injury, Med. Gas Res. 1 (1) (2011) 7.
[8] Y. Gao, Z. Zhuang, S. Gao, X. Li, Z. Zhang, Z. Ye, L. Li, C. Tang, M. Zhou, X. Han, J. Li, Tetrahydrocurcumin reduces oxidative stress-induced apoptosis via the mitochondrial apoptotic pathway by modulating autophagy in rats after traumatic brain injury, Am J Transl Res 9 (3) (2017) 887–899.
[9] W. Li, M.R. Jain, C. Chen, X. Yue, V. Hebbar, R. ZhouA, N. Kong, Nrf2 Possesses a redox-insensitive nuclear export signal overlapping with the leucine zipper motif, J. Biol. Chem. 280 (31) (2005) 28430–28438.
[10] H. Ding, H. Wang, L. Zhu, W. Wei, Ursolic acid ameliorates early brain injury after experimental traumatic brain injury in mice by activating the Nrf2 pathway, Neurochem. Res. 42 (2) (2017) 337–346.
[11] L. Zhang, M. Fei, H. Wang, Y. Zhu, Sodium aescinate provides neuroprotection in experimental traumatic brain injury via the Nrf2-ARE pathway, Brain Res. Bull. 157 (2020) 26–36.
[12] T. Sugiyama, T. Imai, S. Nakamura, K. Yamauchi, S. Sawada, M. Shimazawa, H. Hara, A novel Nrf2 activator, RS9, attenuates secondary brain injury after intracerebral hemorrhage in sub-acute phase, Brain Res. 1701 (2018) 137–145.
[13] K. Ding, H. Wang, J. Xu, T. Li, L. Zhang, Y. Ding, L. Zhu, J. He, M. Zhou, Melatonin stimulates antioxidant enzymes and reduces oxidative stress in experimental traumatic brain injury: the Nrf2-ARE signaling pathway as a potential mechanism, Free Radic. Biol. Med. 73 (2014) 1–11.
[14] U. Wasik, M. Milkiewicz, A. Kempinska-Podhorodecka, P. Milkiewicz, Protection against oxidative stress mediated by the Nrf2/Keap1 axis is impaired in Primary Biliary Cholangitis, Sci. Rep. 7 (2017), 44769.
[15] W. Dai, H. Wang, J. Fang, Y. Zhu, J. Zhou, X. Wang, Y. Zhou, M. Zhou, Curcumin provides neuroprotection in model of traumatic brain injury via the Nrf2-ARE signaling pathway, Brain Res. Bull. 140 (2018) 65–71.
[16] Z. Sun, Y.E. ChinD, D. Zhang, Acetylation of Nrf2 by p300/CBP augments promoter-specific DNA binding of Nrf2 during the antioxidant response, Mol. Cell Biol. 29 (10) (2009) 2658–2672.
[17] Q. Zhao, F. Zhang, Z. Yu, S. Guo, N. Liu, Y. Jiang, E.H. Lo, Y. Xu, X. Wang, HDAC3 inhibition prevents blood-brain barrier permeability through Nrf2 activation in type 2 diabetes male mice, J. Neuroinflammation 16 (1) (2019) 103.
[18] P. Rajendran, W.M. Dashwood, L. Li, Y. Kang, E. Kim, G. Johnson, K.A. Fischer, C.V. Löhr, D.E. Williams, E. Ho, M. Yamamoto, D.A. LiebermanR, H. Dashwood, Nrf2 status affects tumor growth, HDAC3 gene promoter associations, and the response to sulforaphane in the colon, Clin. Epigenet. 7 (1) (2015) 102.
[19] S. Shen, J. Li, P. Casaccia-Bonnefil, Histone modifications affect timing of oligodendrocyte progenitor differentiation in the developing rat brain, J. Cell Biol. 169 (4) (2005) 577–589.
[20] S. Baltan, A. Bachleda, R.S. MorrisonS, P. Murphy, Expression of histone deacetylases in cellular compartments of the mouse brain and the effects of ischemia, Transl Stroke Res 2 (3) (2011) 411–423.
[21] S. Bhaskara, S.K. Knutson, G. Jiang, M.B. Chandrasekharan, A.J. Wilson, S. Zheng, A. Yenamandra, K. Locke, J.L. Yuan, A.R. Bonine-Summers, C.E. Wells, J. F. Kaiser, M.K. Washington, Z. Zhao, F.F. Wagner, Z.W. Sun, F. Xia, E.B. Holson, D. KhabeleS, W. Hiebert, Hdac3 is essential for the maintenance of chromatin structure and genome stability, Cancer Cell 18 (5) (2010) 436–447.
[22] B. Wang, X. Zhu, Y. Kim, J. Li, S. Huang, S. Saleem, R.C. Li, Y. Xu, S. Dore, W. Cao, Histone deacetylase inhibition activates transcription factor Nrf2 and protects against cerebral ischemic damage, Free Radic. Biol. Med. 52 (5) (2012) 928–936.
[23] X. Chen, H. Wang, M. Zhou, X. Li, Z. Fang, H. Gao, Y. Li, W. Hu, Valproic acid attenuates traumatic brain injury-induced inflammation in vivo: involvement of autophagy and the Nrf2/ARE signaling pathway, Front. Mol. Neurosci. 11 (2018) 117.
[24] X. Yang, Q. Wu, L. ZhangL. Feng, Inhibition of histone deacetylase 3 (HDAC3) mediates ischemic preconditioning and protects cortical neurons against ischemia in rats, Front. Mol. Neurosci. 9 (2016) 131.
[25] M. Malvaez, S.C. McQuown, G.A. Rogge, M. Astarabadi, V. Jacques, S. Carreiro, J.R. RuscheM, A. Wood, HDAC3-selective inhibitor enhances extinction of cocaine-seeking behavior in a persistent manner, Proc. Natl. Acad. Sci. U. S. A. 110 (7) (2013) 2647–2652.
[26] R. Matheson, K. Chida, H. Lu, V. Clendaniel, M. Fisher, A. Thomas, E.H. Lo, M. Selim, A. Shehadah, Neuroprotective effects of selective inhibition of histone deacetylase 3 in experimental stroke, Transl Stroke Res 11 (5) (2020) 1052–1063.
[27] Y. Gong, M. Wu, J. Shen, J. Tang, J. Li, J. Xu, B. Dang, G. Chen, Inhibition of the NKCC1/NF-kappaB signaling pathway decreases inflammation and improves brain edema and nerve cell apoptosis in an SBI rat model, Front. Mol. Neurosci. 14 (2021), 641993.
[28] O. Akyol, P. Sherchan, G. Yilmaz, C. Reis, W.M. Ho, Y. Wang, L. Huang, I. Solaroglu, J.H. Zhang, Neurotrophin-3 provides neuroprotection via TrkC receptor dependent pErk5 activation in a rat surgical brain injury model, Exp. Neurol. 307 (2018) 82–89.
[29] Y.T. Chen, X.F. Zang, J. Pan, X.L. Zhu, F. Chen, Z.B. Chen, Y. Xu, Expression patterns of histone deacetylases in experimental stroke and potential targets for neuroprotection, Clin. Exp. Pharmacol. Physiol. 39 (9) (2012) 751–758.
[30] F.H. BardaiS, R. D'Mello, Selective toxicity by HDAC3 in neurons: regulation by Akt and GSK3beta, J. Neurosci. 31 (5) (2011) 1746–1751.
[31] P. Eser Ocak, U. Ocak, P. Sherchan, M. Gamdzyk, J. Tang, J.H. Zhang, Overexpression of Mfsd2a attenuates blood brain barrier dysfunction via Cav-1/Keap-1/Nrf-2/HO-1 pathway in a rat model of surgical brain injury, Exp. Neurol. 326 (2020), 113203.
[32] I.D. Aires, R. Boia, A.C. Rodrigues-Neves, M.H. Madeira, C. Marques, A.F. AmbrósioA, R. Santiago, Blockade of microglial adenosine A(2A) receptor suppresses elevated pressure-induced inflammation, oxidative stress, and cell death in retinal cells, Glia 67 (5) (2019) 896–914.
[33] A.R. Malik, K. Szydlowska, K. Nizinska, A. Asaro, E.A. van Vliet, O. Popp, G. Dittmar, R. Fritsche-Guenther, J.A. Kirwan, A. Nykjaer, K. Lukasiuk, E. AronicaT, E. Willnow, SorCS2 controls functional expression of amino acid transporter EAAT3 and protects neurons from oxidative stress and epilepsy-induced pathology, Cell Rep. 26 (10) (2019) 2792–2804.e6.

[34] C. Li, X. Wang, F. Cheng, X. Du, J. Yan, C. Zhai, J. Mu, Q. Wang, Geniposide protects against hypoxia/reperfusion-induced blood-brain barrier impairment by increasing tight junction protein expression and decreasing inflammation, oxidative stress, and apoptosis in an in vitro system, Eur. J. Pharmacol. 854 (2019) 224–231.
[35] P. Chen, L. Li, Y. Gao, Z. Xie, Y. Zhang, Z. Pan, Y. Tu, H. Wang, Q. Han, X. Hu, X. Xin, β-carotene provides neuro protection after experimental traumatic brain injury via the Nrf2-ARE pathway, J. Integr. Neurosci. 18 (2) (2019) 153–161.
[36] C.A. CobbM, P. Cole, Oxidative and nitrative stress in neurodegeneration, Neurobiol. Dis. 84 (2015) 4–21.
[37] J. Djordjevic, A. Djordjevic, M. Adzic, M. Mitic, I. LukicM, B. Radojcic, Alterations in the Nrf2-Keap1 signaling pathway and its downstream target genes in rat brain under stress, Brain Res. 1602 (2015) 20–31.
[38] E. Barone, F. Di Domenico, C. MancusoD, A. Butterfield, The Janus face of the heme oxygenase/biliverdin reductase system in Alzheimer disease: it's time for reconciliation, Neurobiol. Dis. 62 (2014) 144–159.
[39] Q. Zhao, Z. Yu, F. Zhang, L. Huang, C. Xing, N. Liu, Y. Xu, X. Wang, HDAC3 inhibition prevents oxygen glucose deprivation/reoxygenation-induced transendothelial permeability by elevating PPARgamma activity in vitro, J. Neurochem. 149 (2) (2019) 298–310.
[40] Y. Gong, M. Wu, F. Gao, M. Shi, H. Gu, R. Gao, B.Q. Dang, G. Chen, Inhibition of the pSPAK/pNKCC1 signaling pathway protects the bloodbrain barrier and reduces neuronal apoptosis in a rat model of surgical brain injury, Mol. Med. Rep. 24 (4) (2021).
[41] M.Y. Wu, F. Gao, J.F. Tang, J.C. Shen, R. Gao, B.Q. Dang, G. Chen, Possible mechanisms of the PERK pathway on neuronal apoptosis in a rat model of surgical brain injury, Am J Transl Res 13 (2) (2021) 732–742.
[42] M. Shi, Y. Gong, M. Wu, H. Gu, J. Yu, F. Gao, Z. Ren, M. Qian, B. Dang, G. Chen, Downregulation of TREM2/NF-small ka, CyrillicB signaling may damage the blood-brain barrier and aggravate neuronal apoptosis in experimental rats with surgically injured brain, Brain Res. Bull. 183 (2022) 116–126.
[43] L. Huang, H. Tang, P. Sherchan, C. Lenahan, W. Boling, J. TangJ, H. Zhang, The activation of phosphatidylserine/CD36/TGF-β1 pathway prior to surgical brain injury attenuates neuroinflammation in rats, Oxid. Med. Cell. Longev. 2020 (2020), 4921562.
[44] J. Li, M. Wu, Y. Gong, J. Tang, J. Shen, L. Xu, B. Dang, G. Chen, Inhibition of LRRK2-rab10 pathway improves secondary brain injury after surgical brain injury in rats, Front Surg 8 (2021), 749310.
[45] M. Wu, Y. Gong, L. Jiang, M. Zhang, H. Gu, H. Shen, B. Dang, VEGF regulates the blood-brain barrier through MMP-9 in a rat model of traumatic brain injury, Exp. Ther. Med. 24 (6) (2022) 728.
[46] M. Wu, R. Gao, B. Dang, G. Chen, The blood component iron causes neuronal apoptosis following intracerebral hemorrhage via the PERK pathway, Front. Neurol. 11 (2020), 588548.
[47] P. Gong, R. Li, H.Y. Jia, Z. Ma, X.Y. Li, X.R. Dai, S.Y. Luo, Anfibatide preserves blood-brain barrier integrity by inhibiting TLR4/RhoA/ROCK pathway after cerebral ischemia/reperfusion injury in rat, J. Mol. Neurosci. 70 (1) (2020) 71–83.